Journal of Ovonic Research Vol. 16, No. 3, May - June 2020, p. 181 - 188

STUDY THE OPTICAL PROPERTIES OF THE VARIOUS DEPOSITION SOLUTIONS OF ZnO NANORODS GROWN ON GLASS SUBSTRATE USING CHEMICAL BATH DEPOSITION TECHNIQUE

A. F. ABDULRAHMAN*
Department of Physics, Faculty of Science, University of Zakho, Kurdistan Region, Iraq

In this study, two-step chemical bath deposition (CBD) technique has been employed for the fabrication of Zinc Oxide (ZnO) nanorods at low temperature. The ZnO nano-seed layer was deposited on the glass substrate using a radio frequency sputtering discharge technique. The impact of three zinc salts with Hexamethylenetetramine (HMTA) on the properties of ZnO nanorods have been investigated. The double beam UV visible (UV-4100) spectrometer, micro-Raman scattering, and Field emission scanning electron microscopy (FESEM) were used to characterize and study the optical properties, energy band gap, defects, Raman spectra, phase orientation, quality of material, the interaction of phonons, transport properties, and the morphology of synthesized ZnO nanorods (NRs), respectively. The three zinc salts are Zinc Nitrate Hexahydrate, Zinc Acetate, and Zinc Chloride. The results found that the variation in zinc salts types with Hexamethylenetetramine as deposition solution is play a very important impact on the structures of fabricated ZnO nanorods that effected directly on the optical properties, energy band, material quality, and phase orientation of ZnO NRs. Also, from UV measurement the optical properties and energy band gap of produced ZnO nanorods are changed with changing the zinc salt as a precursor of deposition solution.

(Received March 23, 2020; Accepted June 19, 2020)

Keywords: Optical properties, Various deposition solution, Raman Spectra, ZnO nanorods, CBD

1. Introduction

Recently, nano-sized semiconductors have received wide attention due to its important optical and electrical properties useful in electronic devices and optoelectronic [1]. The ZnO can be prepared in nanostructures with different shapes and dimensions [2]. The ZnO has attracted much attention because of its novel optical and electrical properties. ZnO is an n-type semiconductor with a large direct energy band gap. The band gap of ZnO is 3.37 eV at room temperature and 3.44 eV at low temperatures [3]. These Properties enable ZnO to have more applications in optoelectronic devices, such as in the field of gas sensors, spintronics, solar cells, UV photodetectors, and photocatalysts [4-8]. ZnO can fabricate various nanostructures morphologies such as nanorods, nanowires, nanodisks, flower-like ZnO, tetrapod-like ZnO, and mesoporous [9-14]. There are many synthesized techniques that have been introduced for the growth of a set of ZnO nanorods on the large domain of substrates [15]. These techniques contain radiofrequency magnetron sputtering [16], metallic organic chemical vapor deposition (MOCVD) [17], chemical vapor deposition (CVD) [18], pulsed laser deposition [19], vapor phase transport [20], spray pyrolysis [21] and electrochemical deposition [22]. During these techniques mention above, the chemical bath deposition (CBD) method is a low-temperature technique, and possibly the lowest cost method for growing ZnO nanorods not need the high production yield [23]. The optical properties of ZnO, studied using photoluminescence, photoconductivity, and absorption, reflect the intrinsic direct band gap, a strongly bound exciton state, and gap states due to the point

* Corresponding author: ahmed.abdulrahman@uoz.edu.krd

defects [24]. In previous works, studies were generally focused on the preparation of the ZnO nanorods and growth parameters and solution parameters such as growth time, bath temperature, precursor concentration on the morphology, structure, and the optical of the ZnO nanorods. Also, the deposition solution can influence on the fabrication of the ZnO nanorods because each solution is responsible for the special optical structure and morphology of ZnO nanorods.

In this work, the low-cost CBD method was used to fabricate the ZnO nanorods grown on glass substrates at low temperatures. The impact of the various types of Zinc salts (Zinc Nitrate Hexahydrate, Zinc Acetate, and Zinc Chloride) with HMTA as deposition solutions on the optical properties, energy band gap, defect, Raman spectra, phase orientation, quality of material, the interaction of phonons, transport properties, and morphology of ZnO nanorods were obtained.

2. Experimental details

All chemical materials are from Sigma Aldrich Company and hexamethylenetetramine ($C_6H_{12}N_4$), Zinc Nitrate hexahydrate (Zn $(NO_3)_2.6H_2O$), Zinc Acetate ($Zn(O_2CCH_3)_2(H_2O)_2$) and Zinc Chloride ($ZnCl_2$) were employed as starting materials without further purification. In this paper, the microscopic glass was chosen as substrates and was cleaned in an ultrasonic bath by using ethanol, acetone, and deionized water for 20 min respectively, and dried with nitrogen gas [25]. The 150 nm thick ZnO seed layer was deposited on the glass substrates using a radio frequency magnetron sputtering were employed using target (99.999% purity) with the power of RF sputtering 180 Watt argon gas with pressure 5.8 $*10^{-3}$ mbar for 20 min. Also, the ZnO nano-seed layer that deposited on glass substrates were placed inside in an annealing tube furnace at 300 °C for 2 h. The two-step CBD method has been employed for synthesis of the ZnO NRs. The (Zn $(NO_3)_2.6H_2O$), ($Zn(O_2CCH_3)_2(H_2O)_2$), ($ZnCl_2$), and ($C_6H_{12}N_4$) were utilized as precursors of deposition solutions, and deionized water is used as a solvent. The equal molar 1:1 of HMTA and Zinc Nitrate (sample a) was separately dissolved in deionized water and mixed together under magnetic stirrer to get the homogenous solution [26]. Also, the equal molar concentration of zinc acetate and ($C_6H_{12}N_4$) (sample b) was separately dissolved in de-ionized water and mixed under magnetic stirrer. In addition, the equal molar concentration of zinc chloride and ($C_6H_{12}N_4$) (sample c) was separately dissolved in de-ionized water and mixed together under magnetic stirrer. The prepared samples are vertically placed separately into three containers (beaker) includes a mixture of the two deposition solutions for three cases. To obtain the impact of three different zinc salts as precursors of deposition solution on the optical properties, energy band gap, Raman spectra, phase orientation, material quality, and morphology of ZnO NRs. Three containers were placed inside a laboratory oven at 90 ^oC for 3 h. After finish the required time of growth of the ZnO NRs, the samples were first taken out from a solution and washed with de-ionized water to eject the remaining salt, and then it was dried with nitrogen gas. The optical properties, energy band, Raman activity, phase orientation, material quality and morphology of synthesized ZnO NRs from different Zinc Salts are studied and examined by using a double beam UV visible (UV-4100) spectrometer with a wavelength range 300 nm to 800 nm, Raman spectroscopy system (model: HR 800 UV, HORIBA Jobin Yvon, and Edison USA) and the model of FESEM used in this study is: FEI Nova nano SEM 450 (The Netherlands), and Leo-Supra 50 VP, Carl Zeiss (Germany), respectively.

3. Results and discussion

The optical properties of ZnO nanorods grown from different deposition solutions are studied based on observation of the optical transmissions and absorptions through the ZnO nanorods films using UV-Vis spectrometers. Figure 1 shows the effect of the various deposition solutions on the optical transmittance spectrum of ZnO nanorods fabricated at 90˚C using UV-Visible spectroscopy with wavelength ranged from 300 nm to 800 nm. It is obtained that the most fabricated ZnO nanorods samples in the visible region have high transmittance and low transmittance in the UV region. The higher transmittance is found over 16% in the visible region

from 400 nm to 800 nm for ZnO nanorods films grown from Zinc Nitrate Hexahydrate: HMTA, which is decreased to 4% and 0.7% for ZnO nanorods produced from Zinc Acetate: HMTA, and Zinc Chloride: HMTA, respectively. This may essentially be due to promoted scattering effect in ZnO nanorods films grown from Zinc Chloride effect [27], and higher thickness (length) of ZnO nanorods thin film which have large hexagonal grain size and larger surface roughness [28], and for Zinc Chloride due to the increases the optical scattering which reduces the transmittance of the thin films [28, 29]. The higher thickness of ZnO thin films is due to the higher absorption. The absorption coefficient can increase with the presence of oxygen vacancies [28]. The transmittance decreases sharply near the UV region at a wavelength around 389 nm. From figure 1 (c), the thin films were observed a shorthand in the optical transmittance spectrum this is due to the scattering at grain boundaries [28, 30]. The smaller crystalline size of ZnO nanorods led to increases in the transmittance of ZnO thin films due to decreases the optical scattering [31]. The transmission spectra are shifted to longer wavelengths for all prepared samples that means the optical properties of obtained ZnO nanorods have been changed [29, 32]. The shift of the absorption edge to higher wavelength was caused by the reduction of the transition distance between energy levels usually called band gap energy [32], and may be attributed to the internal stress produced in the film and the light scattering effects in the films caused by the random distribution of the NRs arrays [29].

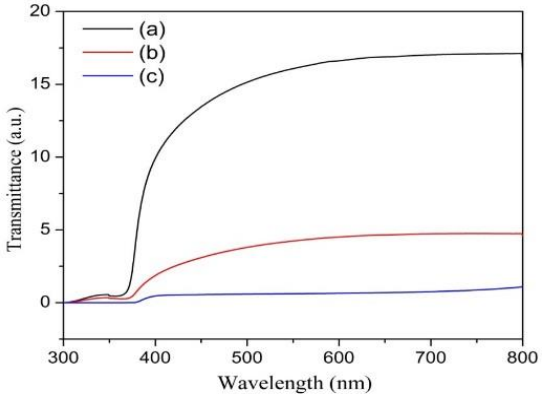

Fig. 1. Optical Transmission Spectrum of ZnO Nanorods for Various Deposition Solutions (a) Zinc Nitrate Hexahydrate, (b) Zinc Acetate and (c) Zinc Chloride.

The optical absorption spectrum of the ZnO nanorods prepared from three various deposition solutions for 3 h with a wavelength range between 300 nm to 800 nm as shown in Figure 2. It can clearly see that the absorbance spectrum reveals the strong absorption high absorbance in the UV region at wavelength below 400 nm and high transparency low absorbance in the visible region, which are the characteristics of ZnO [33]. The low absorption values at long wavelengths are regarded to the impurities of the ZnO nanorods thin film such as interstitial Zn atoms and oxygen vacancies, which act as donor defects [34]. The sharp UV absorption edge and exciton absorption was observed in the range (384-399) nm, which is corresponding to the optical energy band gap of the ZnO nanorods, The sample (2c) shows the highest absorption at highest wavelength while the sample (2a) has the lowest absorption at the lowest wavelength it means the optical properties have been changed, and this is because of the topography, nature, and structure of ZnO nanorods which have small space between nanorods. These spaces give chance to high transmitted less absorption of intensity. Also, the sample (2a) has a large space or small diameter and short length of the ZnO nanorods compare to the sample (2b) & (2c).

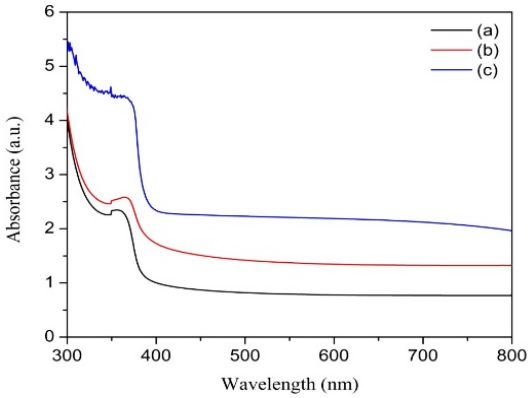

Fig. 2. Optical Absorption Spectrum of ZnO Nanorods for Various Deposition Solution (a) Zinc Nitrate Hexahydrate, (b) Zinc Acetate and (c) Zinc Chloride.

The optical energy band gap of ZnO nanorods fabricated by CBD is calculated from the transmission and absorption spectrum by the extrapolation of the linear portion of $(\alpha h\nu)^2$ versus hν plots using Tauc formula [35, 36]:

$$(\alpha h\nu)^2 = A(h\nu - E_g)^n \quad (1)$$

where α is the absorption coefficient, hν is the photon energy, A is constant, Eg is the optical energy band gap and n depends on the transmission type (equals to 1/2 for allowed direct transmission and 2 for indirect transition). It known that the zinc oxide (ZnO) is direct transition semiconductor, and then the value of n is ½ [35].

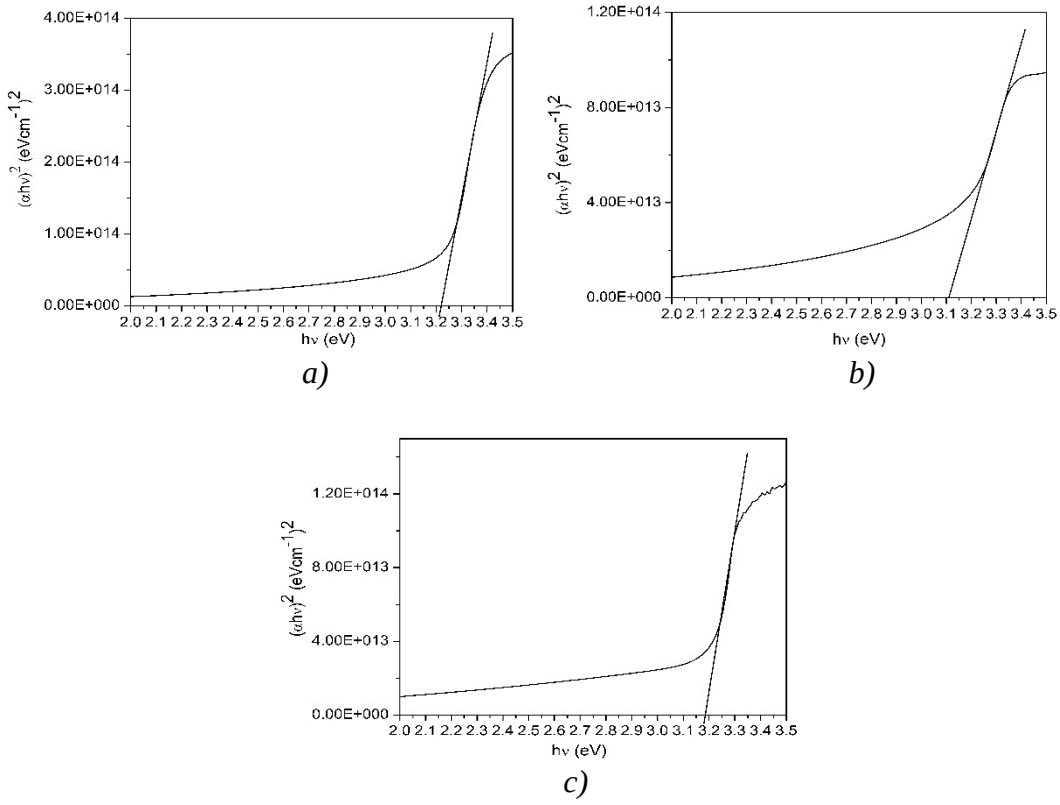

Fig. 3. Tauc plot $(\alpha h\nu)^2$ Versus Energy Band Gap (hν) of the ZnO Nanorods for Different Deposition Solution (a) Zinc Nitrate Hexahydrate, (b) Zinc Acetate and (c) Zinc Chloride.

The Tauc plot $(\alpha h\nu)^2$ versus the energy band gap ($h\nu$) of the ZnO nanorods grown for various deposition solution is shown in Figure 3. The plots are clearly show that the transition region approximately 3.2 eV, and it corresponds to the direct transition band between the edges of valance and conduction bands which represent the optical energy gap of ZnO semiconductor [33]. Regarding the plot, it exactly investigated the band gap energy of ZnO nanorods are about 3.221 eV, 3.11 eV, and 3.18 eV for Zinc Nitrate Hexahydrate, Zinc Acetate and Zinc Chloride, respectively. This agrees with literature for single crystal ZnO [37]. The energy band gap (E_g) is concerned with the carrier concentration, stress state and grain size in the material [37]. The maximum of energy band gap for the ZnO nanorods grown from Zinc Nitrate Hexahydrate may be related to the small grain size. Also, the minimum energy band gap is found of ZnO nanorods prepared from Zinc acetate grain size, a decrease of carrier concentration, the tensile stress, and oxygen vacancies which lead to the decrease of the carrier concentration in the conduction band [38, 39].

The micro-Raman scattering is one of the non-destructive and contactless studies and subsequently it does not need any special preparation of the sample for measurements. It is an effective tool to examine (analyze) the phase orientation, quality of material, interaction of phonons, and transport properties [38]. Wurtzite ZnO belongs to the space group of C_{6v}^4 which predicts that the eight sets of phonon modes are observable at wave vector $k \approx 0$ (Γ point). In the eight phonon modes of ZnO, six of them are optical phonon modes, and the remaining two phonon modes are acoustic. According to group theory, the optical mode at the Γ point of the Brillouin zone can be represented by [40, 41].

$$\Gamma = 1A_1 + 2B_1 + 1E_1 + 2E_2 \quad (2)$$

Among these modes, the $1A_1$, $1E_1$, and $2E_2$ modes are Raman active. The A_1 and E_1 mode are infrared active and only E_2 modes is Raman Active. The $2B_1$ modes are silent modes. Both A_1 and E_1 mode are split into transverse optical (TO) and longitudinal optical (LO) phonons. Non-polar phonon modes with E_2 symmetry separate into two frequencies; $E_{2(high)}$ modes are associated with oxygen atoms and $E_{2(low)}$ modes are associated with Zn sub-lattice. Because the Raman scattering is perpendicular to the c-axis of ZnO nanorods, so only $E_{2(high)}$ and $A_{1\ LO}$ are Raman active [42].

In the present study, the effect of the various deposition solutions on the Raman spectroscopy is investigated. Figure 4 shows the typical Raman spectra of ZnO nanorods grown on glass substrates for different deposition solutions. The appearance of dominant and sharp peaks at approximately 100 cm^{-1} and 437 cm^{-1} for the ZnO nanorods grown from all deposition solutions, which corresponds to the intrinsic characteristics of the Raman active $E_{2(low)}$ and $E_{2(high)}$ modes of the hexagonal wurtzite ZnO, respectively. The existence of a sharp and dominant peak of $E_{2(High)}$) mode without $E_{2(Low)}$ mode confirms that the grown ZnO nanorods have a hexagonal wurtzite structure with a good crystal quality [43].

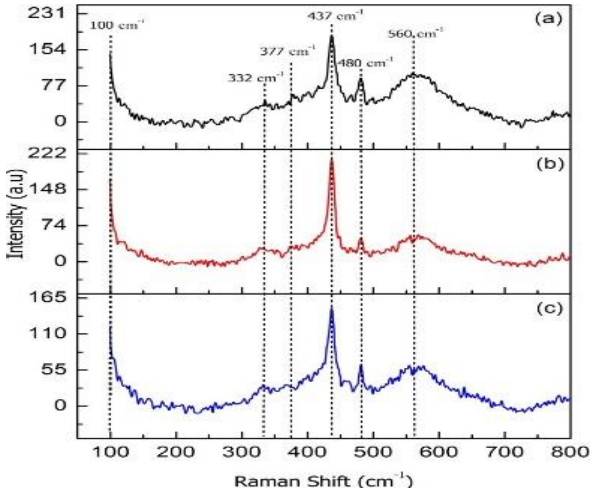

Fig. 4. Typical Raman Spectra of the ZnO Nanorods for Various Deposition Solutions (a) Zinc Nitrate Hexahydrate, (b) Zinc Acetate and (c) Zinc Chloride.

The weak peaks at approximately 332 cm^{-1} which is associated with $E_{2(high)}$ - $E_{2(low)}$ (multiple phonon process), and the $A_{1\ (TO)}$ mode is showed around 377 cm^{-1} are observed for the ZnO nanorods grown for all samples [38, 44]. The peaks 480 cm^{-1}, 560 cm^{-1}, and 580 cm^{-1} are corresponding to the $E_{1(Low)}$ mode to impurities and structural defects (oxygen vacancies and Zn interstitials). The intensities of the ZnO Raman active peak of ZnO nanorods that were grown from Zinc Acetate become higher as the ZnO nanorods grown from other deposition solution, which indicates the increase in the crystal quality of the nanorods and/or the increase in the coverage of the nanorod arrays on the substrate [44].

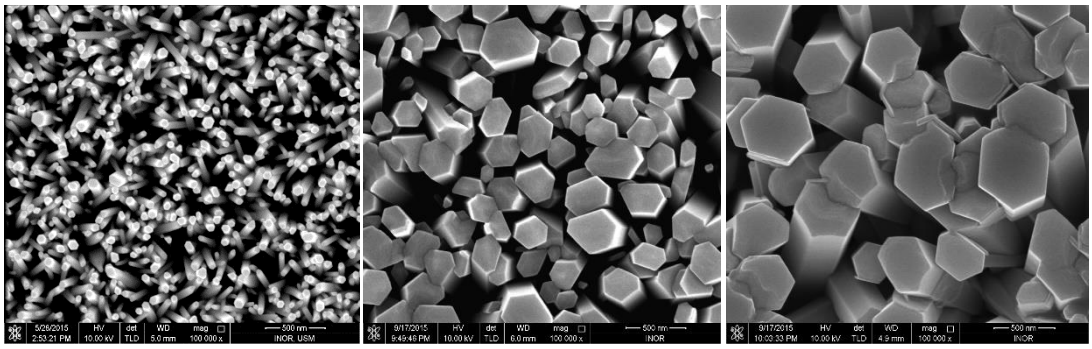

a) *b)* *c)*

Fig. 5. Surface Topography FESEM Images of the ZnO Nanorods for Various Deposition Solutions (a) Zinc Nitrate Hexahydrate, (b) Zinc Acetate and (c) Zinc Chloride.

The surface topography such as size, shape, distribution, aligned and homogeneity of the ZnO NRs prepared from various types of zinc salts as deposition solution are shown in Figure 5. The ZnO NRs synthesized from Zinc Nitrate Hexahydrate with HMTA as the precursor of deposition solution is shown in Figure (5a), and it can clearly see that the ZnO NRs have grown with high distribution, uniform orientation, uniform size, high density, and vertically well-aligned over an entire glass substrate with an average diameter of 91 nm. In the case of ZnO NRs produced from ($Zn(O_2CCH_3)_2(H_2O)_2$): ($C_6H_{12}N_4$), the average diameter was increased to 331 nm as shown in Figure (5b). It was observed that the ZnO NRs were oriented randomly and highly density distribution. Also, the obtained ZnO NRs have non-uniform size, have a hexagonal shape, have no same high, and most NRs has grown like the group. Figure (5c) shows the ZnO NRs synthesized from the precursor of deposition solution ($ZnCl_2$): ($C_6H_{12}N_4$). It can clearly see that the ZnO NRs

have a perfect hexagonal shape with uniform orientation, and most obtained ZnO nanorods or micro-rods growth like group or set of rods with an average diameter of 529 nm.

4. Conclusions

Vertically well-aligned ZnO nanorods are successfully fabricated using two-step CBD technique at 90 °C. The effect of the various zinc salts: HMTA as the precursor of deposition solution on the optical properties (absorbance and transmittance), energy band gap, Raman activity, material quality, phase orientation, surface topography, size, homogeneity, distribution, and density of ZnO NRs were investigated. The results investigated that the different zinc salts with HMTA as precursors of deposition solution have a very clearly and crucial impact on optical properties, energy band gap, Raman activity, phase orientation, and morphology of ZnO nanorods.

Acknowledgements

The author wishes to gratefully thank the University of Zakho, Kurdistan Region-Iraq for their support of this work.

References

[1] S. S. Dange, S. N. Dange, P. S. More **2**(10), 2015.
[2] W. K. Tan et al, Journal of Solid State Chemistry, **211**, 146 (2014).
[3] A. F. ABDULRAHMAN, S. M. AHMED, N. M. AHMED, M. A. ALMESSIERE, Digest Journal of Nanomaterials and Biostructures, **11**(3), 1007 (2016).
[4] T. Meron, G. Markovich, J. Phys. Chem. B. **109**, 20232 (2005).
[5] X. L. Cheng et al, Sensors and Actuators B **02**(2), 248 (2004).
[6] Y. Hames et al., Solar Energy **84**(3), 426 (2010).
[7] P. Sharma, K. Sreenivas, K. V. Rao, Journal of Applied Physics **93**(7), 3963 (2003).
[8] P. V. Kamat et al., Journal of Physical Chemistry B **106**(4), 788 (2002).
[9] M. A. Shah, F. M. Al-Marzouki **1**, 77 (2010).
[10] C. X. Xu et al., Applied Physics Letters **85**, 3878 (2004).
[11] L. Luo, B. D. Sosnowchik, L. Lin, Applied Physics Letters **90**, 1 (2007).
[12] R. Wahab, S. G. Ansari, H.-K. Seo et al., Solid State Sciences **11**, 439 (2009).
[13] J. Cheng, R. Guo, Applied Physics Letters **85**, 5140 (2004).
[14] Weidong Yu, Xiaomin Li, Xiangdong Gao, Crystal Growth & Design **5**, 151 (2005).
[15] Huang et al., J. Electrochem. Soc. **158**, 38 (2011).
[16] J. Y. Lee, Y. S. Choi, J. H. Kim, M. O. Park, S. Im, Thin Solid Films **403**, 553 (2002).
[17] D. Montenegro et al., J. Appl. Phys. **113**, 143513 (2013).
[18] P. Yang et al., Advance Functional. Material **12**, 323 (2002).
[19] J. H. Choi, H. Tabata, T. Kawai, J. Cryst. Growth **226**, 493 (2001).
[20] C. X. Xu, X. W. Sun, Z. L. Dong, M. B. Yu, Appl. Phys. Lett. **85**, 3878 (2004).
[21] M. G. Ambia, M. N. Islam, M. O. Hakim, J. Mater. Science **29**, 6575 (1994).
[22] H. H. Guo, J. Z. Zhou, Z. H. Lin, Electrochem. Commun. **10**(1), 146 (2008).
[23] Abdulrahman, A., Ahmed, S., & Ahmed, N., Science Journal of University of Zakho, 5(1), 128-135, (2017)
[24] L. Wu, Y. Wu, X. Pan, F. Kong, Optical Materials **28**, 418 (2006).
[25] A. F. ABDULRAHMAN, S. M. AHMED, N. M. AHMED, M. A. ALMESSIERE, Digest Journal of Nanomaterials and Biostructures, **11**(4), 1073 (2016).
[26] Ahmed F Abdulrahman, Sabah M. Ahmed, Naser M. Ahmed, Munirah A. Almessiere, AIP Conference Proceedings, **1875**(1), 020004 (2017).
[27] R. N. Gayan et al., Indian Journal of Pure and Applied Physics **48**, 385 (2010).

[28] C. C. Ting et al.,Thin Solid Films **518**, 4156 (2010).
[29] M. F. Malek et al, Japanese Journal of Applied Physics **55**, 01AE15 (2016).
[30] J. H. Lee, I. C. Leu, M. H. Hon, Journal of Crystal Growth **275**, 2069 (2005).
[31] K. C. Yung, H. Liem, H. S. Choy, J. Phys. D **42**, 185002 (2009).
[32] Akhiruddin, I. Sugianto, Journal of Materials Physics and Chemistry **2**(2), 34 (2014).
[33] L. Roza et al., Journal of Alloys and Compounds **618**, 153 (2015).
[34] Kurniawan Foe et. Al., ECS Transactions **25**(24), 3 (2010).
[35] Abdulrahman, A., Ahmed, S., & Ahmed, N., Science Journal of University of Zakho, 6(4), 160 (2018).
[36] X. L. Zhang et al, Cryst. Res. Technol. **49**(4), 220 (2014).
[37] A. K. QASIM, L. A. JAMIL, A. F. ABDULRAHMAN, Digest Journal of Nanomaterials and Biostructures, **15**(1), 157 (2020).
[38] A. F. ABDULRAHMAN, S. M. AHMED, M. A. ALMESSIERE, Digest Journal of Nanomaterials and Biostructures, **12**(4), 1001 (2017).
[39] Abdulrahman AF, Ahmed SM, Ahmed NM, Almessiere MA., *Crystals*. **10**(5), 386 (2020)
[40] W. B. Mi, H. L. Bai, H. Liu, C. Q. Sun, J. Appl. Phys. **101**, 023904 (2007).
[41] H. M. Zhong et al., J. Appl. Phys. **99**, 103905 (2006).
[42] F. Decremps et al., Phys. Rev. B **65**, 092101 (2002).
[43] N. I. Rusli et al., Materials **5**, 2817 (2012).
[44] W. K. Tan et al., Journal of Solid State Chemistry **211**, 146 (2014).